ACS APPLIED MATERIALS & INTERFACES

Letter

www.acsami.org

Capillary Wave Confinement-Induced Stabilization of Polymer Films

Diya Bandyopadhyay,[†] Gurpreet Singh,[†] Matthew L. Becker,[‡] and Alamgir Karim*,[†]

[†]Department of Polymer Engineering and [‡]Department of Polymer Science, The University of Akron, Akron, Ohio 44325, United States

Supporting Information

ABSTRACT: We show that temporary confinement of polystyrene thin films by an elastomeric capping layer possessing nanoimprinted subcapillary wavelength ($\lambda \ll \lambda_{cap}$ (20 μm)) line channels (amplitude $A \approx 120$ nm) can suppress film dewetting on thermodynamically unfavorable substrates by arresting the amplitude growth and in-plane propagation of the destabilizing surface capillary waves. Confinement by either a smooth elastomer capping layer ($A \approx 1$ nm) or with pattern features above the threshold dimension only retards dewetting but does not prevent it. The nanoimprint pattern is therefore essential to preventing dewetting, illustrating that only the penalty of elastomer deformation and interfacial tension reduction is insufficient.

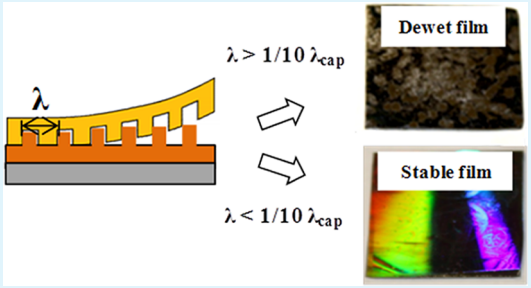

KEYWORDS: *dewetting, polymer films, nanopattern, flexible confinement, capillary wave*

Nanopatterning of polymer thin films by soft nanoimprinting methods is a growing area of significant technological importance such as polymer solar cells.[1,2] Yet, progress toward practical applications of such functional polymer thin films has been impeded to date because of the persistent issue of thin film dewetting during thermal processing above the polymer glass transition temperature.[3,4] As film thicknesses approach molecular dimensions, antagonistic short-range and long-range forces lead to the amplification of destabilizing surface perturbations in the form of capillary fluctuations, which in turn greatly affect film dynamics and stability. From the point of view of surface hydrodynamics of thin liquid films, it was proposed by Scheludko[5] that at a critical film thickness $h_c = (3K\lambda^2/64\sigma)^{0.25}$ (λ is the characteristic wavelength of the surface fluctuation; K is related to the Hamaker constant, $A = 6\pi/K$; and σ is the surface tension) confinement effects lead to the domination of van der Waals (VDW) forces and surface tension forces over gravitational effects, thus differentiating thin film (h < 100 nm) dynamics from bulk films. Spontaneous dewetting of liquid thin films then takes place driven by a spectrum of capillary waves $\zeta(x, y) = \sum A(q)e^{iqs}$, q and $A(q)$ being the wavevector and amplitude of each capillary wave and s a vector in the (x, y) plane.[6] Numerical solutions of nonlinear equations of motion have estimated the length scale of the fastest growing (dominant) mode of the instability, λ_{cap}, for a thin liquid film, to be related to the destabilizing force $\varnothing''(h)$ as $\lambda_{cap}(h) = [-4\pi^2\sigma/\varnothing''(h)]^{0.5}$, where h is the film thickness.[7] In thick films, thermally induced capillary waves on polymer surfaces have an amplitude $A(q) = \sqrt{\langle(\Delta z)^2\rangle}[k_bT/2\pi\sigma]\ln\{\lambda_{max}/\lambda_{min}\} \approx$ 0.1−1 nm.[8,9] Here, λ_{max} and λ_{min} are the maximum and minimum wavelengths of the capillary wave fluctuations. Thus we note that the amplitude of the capillary waves is related to their wavelength spectrum. For wetting films of thicknesses 5−50 nm, dispersive effects further reduce the capillary amplitude.[8,9] However, for nonwetting films of these thicknesses, the amplitude of the unstable wave builds up and ultimately leads to film dewetting. The fundamental question that we investigate here is, if the dominant surface capillary wavelength of the polymer, $\lambda_{cap} = \zeta(x, y)_{max}$ is confined by means of a physical confinement that is capable of restricting its propagation dynamics, would the film retain its stability on an otherwise unfavorable substrate. Previously, Kargupta et al.[10] have shown via simulations that a polymer thin film on a chemically heterogeneous substrate with 1D stripe width less than the characteristic instability wavelength leads to wetting of the film on the substrate in order to avoid an otherwise high surface energy penalty. This phenomenon in 2D can be anticipated more readily because of the symmetry of the capillary wave, $\zeta(x, y)$, but even in this case, confinement induced wetting is only nominally documented. Lee et al.[11] have demonstrated that polymer film confinement by 2D features can lead to directed dewetting via capillary force lithography or a wetting film depending on the feature dimensions relative to the instability length scale. However, a systematic study elucidating the effects of simultaneous pattern wavelength and amplitude of 1D confinement on polymer thin film stability and resultant influence of pattern-polymer interfacial energy and mechanical considerations on capillary dynamics is lacking. 1D confinement is fundamentally intriguing because the capillary waves are confined only in the lateral direction but experience no confinement in the transverse direction.

Received: January 19, 2013
Accepted: April 12, 2013
Published: April 12, 2013

   dx.doi.org/10.1021/am4002502 | ACS Appl. Mater. Interfaces 2013, 5, 4006−4010

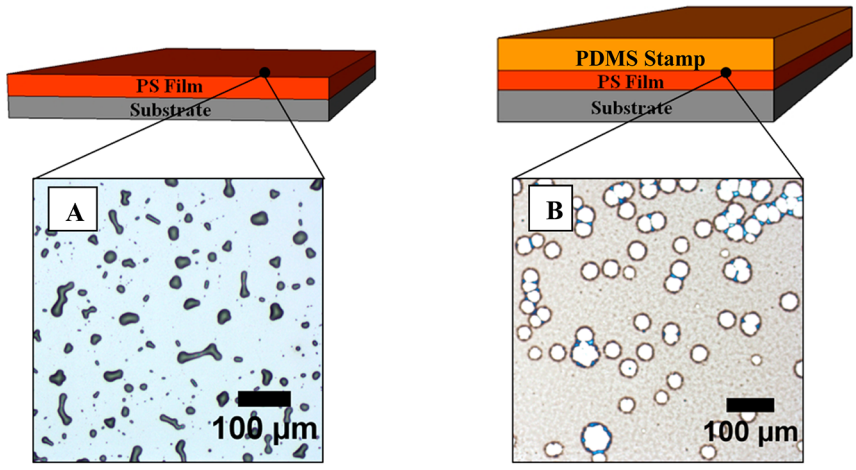

Figure 1. Effect of top-down flexible, unpatterned confinement on PS film stability against dewetting (A) Representative optical image of a late-stage dewet PS film (120 nm) on a quartz substrate annealed at 140 °C for 24 h under vacuum (B) Representative optical image of an early stage smooth PDMS-capped dewetting PS film (120 nm) upon annealing at 140 °C for 24 h under vacuum, quenched rapidly to room temperature.

In this paper, we present a facile strategy to suppress the fundamental film destabilization process of capillary driven dewetting by confining the surface capillary waves via a top-down 1D nanopatterned soft confinement approach. Such a method would not only provide a means of obtaining stable polymer thin films with minimal system alterations, unlike existing strategies that involve significant modifications to the polymer and/or substrate,[12−15] but also enable the fabrication of large - area stable nanopatterned coatings. We systematically design and study regimes of patterned confinement with one-dimensional channels of pitch ($\lambda_{pattern}$) and amplitude ($A_{pattern}$), such that the dimensions vary systematically from $\lambda_{pattern} > \lambda_{cap}$ to $\lambda_{pattern} \ll \lambda_{cap}$ and from $A < h$ to $A > h$. Their effects on a well-defined and widely used model polystyrene (PS) film system on silicon and silica (quartz) substrates, which PS typically dewets is reported. Unentangled, short-chain PS thin films are employed in our studies to demonstrate the stabilization effect in polymer systems that are known to exhibit rapid dewetting kinetics. The stability of PS on SiO can be predicted from the effective interface potential ($\emptyset(h)$) which is a function of initial film thickness (h) and incorporates short-range and long-range interactions as: $\emptyset(h) = c/h^8 - A_{eff}/12\pi h^2$, where c is a measure of the short-range interactions and A_{eff} is the effective Hamaker constant of PS on SiO system confined by PDMS, given by $(\sqrt{A_{SiO}} - \sqrt{A_{PDMS}})(\sqrt{A_{air}} - \sqrt{A_{PDMS}})$. If $\emptyset''(h)$ is negative, the PS film on the SiO_2 substrate is unstable because of the propagation and amplification of the most dominant mode of the capillary wave. The propagating wavelength of the dominant capillary instability (λ_{cap}) of PS can be evaluated from the expression of $\emptyset(h)$ introduced in the previous section. At our experimental annealing temperatures of 140 °C, the values of c, A_{eff}, and σ are, $c \approx 6 \times 10^{-76}$ J m,[6] $A_{eff} \approx 1 \times 10^{-20}$ J, and $\sigma \approx 35$ mN/m. Under these conditions, ultrathin PS films are unstable ($f''(h) < 0$) and can rupture via spinodal dewetting. The calculated capillary wavelength $\lambda_{cap} \approx 20$ μm for a 40 nm PS film on SiO_2,[16] which is in good agreement with our experimentally observed average dewetting hole-to-hole distance of ∼22 μm for thin unconfined PS films. We note the value of λ_{cap} would have been much smaller, had we estimated it from the post patterning film residual layer thickness. However, it can be shown that the time required to fill the channel by PS estimated as $t_{fill} = 2\eta z^2/R\sigma\cos\theta \approx 2$ s,[17] (where η − polymer viscosity; z, pattern height, R, hydraulic radius, and θ, contact angle at polymer-mold interface) is much greater than the spontaneous instability growth and propagation time ∼1 ms,[18] so that the effective λ_{cap} calculated from residual thickness might not be an accurate estimate.

We start with illustrating the effect of the zeroth order confinement by a smooth (unpatterned) polydimethylsiloxane (PDMS) layer, with effectively $\lambda_{pattern} = \infty$ and $A_{pattern}$ (surface roughness) = 1 nm. For such a system, we may anticipate that the natural dewetting of PS would be affected due to two effects. The elastic bending energy penalty of the confining PDMS layer would resist deformation and PDMS contact would also alter the interfacial energetics. Elastomeric masks were prepared using polydimethylsiloxane (PDMS), Sylgard 182 cured onto patterned templates. The resultant pattern dimensions created were (a) pitch (λ) = 40 μm; and amplitude (A) = 40 μm; (b) λ = 1.5 μm and A = 120 nm; (c) λ = 750 nm and A = 120 nm. Polystyrene (PS) (Polymer Source Inc.) of molecular weight 3000 g/mol and molecular weight distribution (M_w/M_n) of 1.09 was spin coated onto clean silicon wafers to yield films of thicknesses ranging from 30 to 250 nm by varying spin coater RPM from 10,000 to 2,000. Patterned and unpatterned PDMS sheets were placed on the PS films without the application of any external pressure and the PS-PDMS sandwich systems were annealed at 140 °C for 24 h. PS thin film confinement by a smooth (unpatterned) polydimethylsiloxane (PDMS) layer shows a typical late-stage dewetting pattern of a 120 nm PS thin film on SiO (Figure 1A). In contrast, upon confining this system by a 1 mm thick unpatterned PDMS film (Figure 1B) and thermally annealing identically to the unconfined PS film, the capillary instabilities give rise only to holes seen in early stages of dewetting. Both energetics and mechanics of a confining surface are involved here. PDMS has a surface energy of ∼20 mJ/m^2, whereas low M_w PS ∼ 35 mJ/m^2, so that if we had a layer of PS on PDMS, the surface energetics given by the spreading parameter, S, for PS to wet PDMS is unfavorable, i.e. S < 0, which is also true for

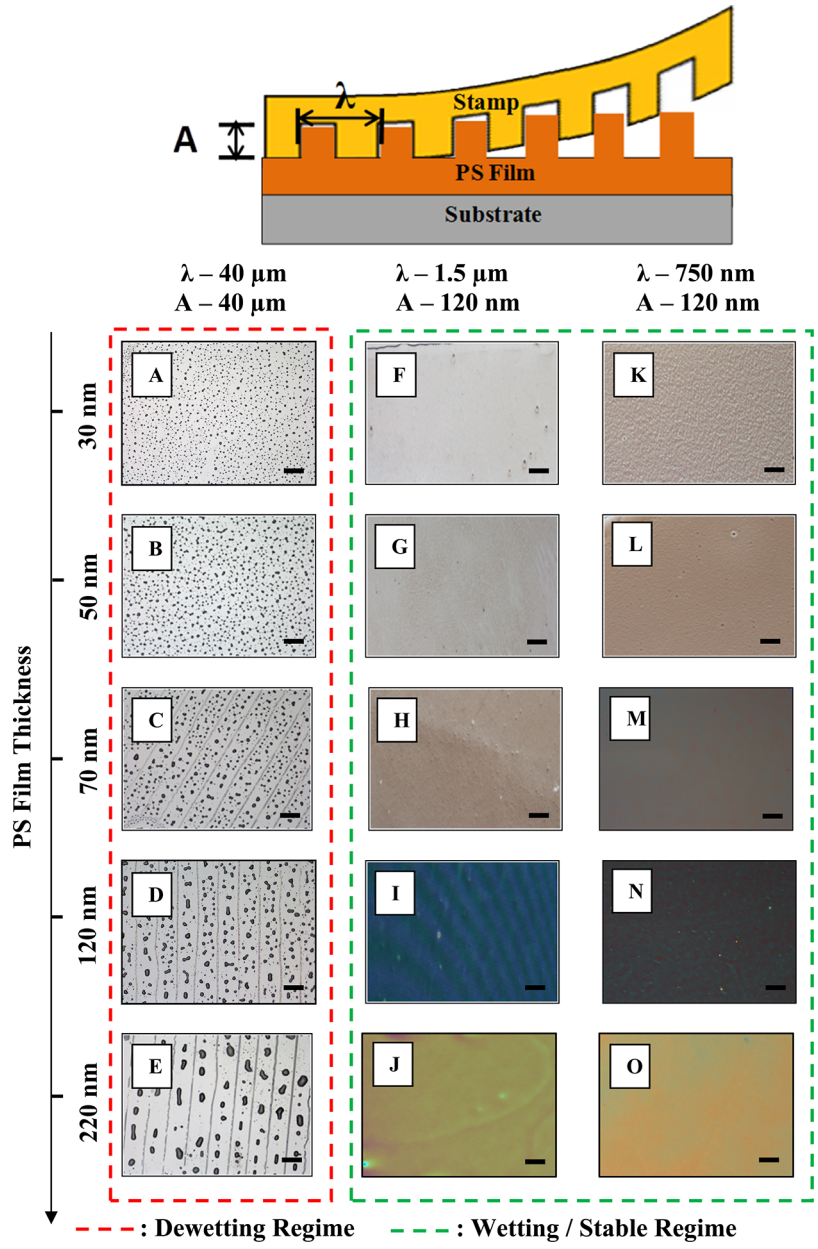

Figure 2. Effect of top-down flexible, patterned confinement and variable length scales of pattern dimensions on PS film stability on silicon as a function of PS film thickness (A–E) Representative optical micrographs of late-stage dewet PS films of thicknesses 30, 50, 70, 120, and 220 nm, respectively, confined during annealing by a patterned PDMS sheet of pattern dimensions 40 μm (λ) and 40 μm (A) followed by removal of confinement after quenching to room temperature rapidly. Representative optical images of stable and wetting PS films of increasing thicknesses (30, 50, 70, and 120 nm respectively) confined during annealing with patterned PDMS sheets of dimensions (F–J) 1500 nm (λ) and 120 nm (A) and (K–O) 750 nm (λ) and 120 nm (A). Following the annealing protocol, the films were quenched rapidly to room temperature and the confining PDMS was removed. Subcapillary wavelength confinement yields completely stable films at all thicknesses; whereas, confinement by pattern dimensions > λ_{cap} gives rise to directional dewetting. Scale bars, 50 μm.

the sandwich system of PDMS/PS/SiO (quartz). The gain in interfacial energy is then dissipated in the liquid rim of the hole considering the PDMS is purely elastic. Brochard et al.[19] have shown that using lubrication approximation and energy balance per unit time, the free energy change of the system as a result of intercalation of the polymer film in the liquid state by the elastomer layer and substrate, is given by $\Delta F_{confinement} = SR^2 + E(h/R)^2R^3$; where S is the spreading parameter, R the radius of the dewet hole, and E the modulus of the elastomer. The first term gives the surface energy gained to create a hole of radius R, which competes with the elastic energy of deformation (second term). For our system, the surface energy gained per unit area to form a hole (5.8×10^{-12} N m) is estimated to be 2 orders of magnitude greater than the elastic deformation energy per unit interfacial area created (5.2×10^{-14} N m), thus explaining the presence of dewetting holes under unpatterned confinement. The retarded kinetics of dewetting is attributed to the imposed mechanical confinement via PDMS elasticity and reduced interfacial driving force for dewetting which limits holes growth. These holes are unable to interconnect and transform to typical late-stage dewet droplet structures with

dx.doi.org/10.1021/am4002502 | ACS Appl. Mater. Interfaces 2013, 5, 4006–4010

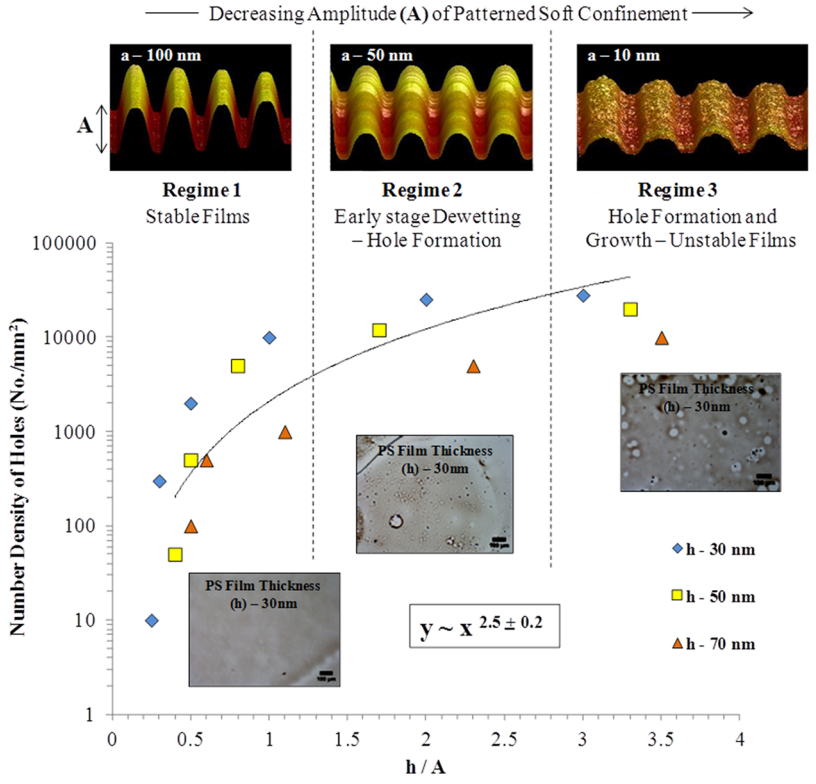

Figure 3. Effect of confining pattern amplitude on PS film stability. A plot of number density of holes (direct measure of film stability) versus the ratio of initial film thickness (h) to the confining pattern amplitude (A). Scale bars, 100 μm.

extended annealing time, suggesting an energy balance, $\Delta F_{\text{dewetting}} = \Delta F_{\text{confinement}}$ once the initial holes are formed.

When $\lambda_{\text{pattern}} \geq \lambda_{\text{cap}}$, it is anticipated that the film would dewet with retarded kinetics due to the propagation of surface capillary waves between the pattern features in conjunction with the confinement effect of the high elastic energy penalty required for deformation of the confining PDMS. We may then anticipate that when $\lambda_{\text{pattern}} \ll \lambda_{\text{cap}}$, the natural dewetting wavelength of PS would be further retarded and perhaps even suppressed due to the interruption of propagation of the capillary wave by the subcapillary wavelength patterns. Indeed, there exist studies that reveal that when $\lambda_{\text{pattern}} \approx$ tens of micrometers, directed dewetting occurs, a phenomenon commonly referred to as capillary force lithography.[2,11,20−22] Figures 2A−E show optical micrographs of PS films of thicknesses 30, 50, 70, 120, and 220 nm, respectively, confined by patterned PDMS masks having channel grating dimensions of 40 μm pitch (λ) and 40 μm amplitude (A) annealed at 140 °C for 24 h. At these scales, on the order of capillary wavelength values of confinement in one dimension, the surface instabilities on the PS film can propagate without any apparent constraints, and with time, amplify leading to late-stage dewetting. The dewetting droplets are well aligned along the confining pattern features, analogous to structures obtained via capillary force lithography.

In contrast, reducing the 1D confining channel dimensions substantially to ∼1/20th of capillary wavelength while maintaining $A_{\text{pattern}} > h$ dramatically prevents dewetting! The confining pattern acts to fully suppress the amplification of the surface instability waves and the pattern feature edges apparently act as truncation edges for the capillary waves as shown in Figure 2F−O. Optical micrographs of PS thin films spanning thicknesses from 30 nm to 220 nm confined by patterned PDMS gratings of dimensions 1.5 μm pitch (λ) and 120 nm amplitude (A) (figures 2 F−J) as well as gratings of dimensions 750 nm pitch (λ) and 120 nm amplitude (A) (figures 2 K−O) demonstrate complete PS film stability upon annealing under these nanoimprint confinement. It is thus evident that there exists a critical 1D confining pattern $\lambda_{\text{critical}}$ much below the capillary wavelength regime, $\sim\lambda_{\text{cap}}/20$, where the destabilizing film surface capillary dynamics are suppressed sufficiently to prevent film dewetting.

As discussed in the previous section, when the capillary amplitude $A_{\text{cap}}(q) \approx h$, dewetting can initiate given that confinement by a smooth PDMS sheet did not suppress dewetting and the PDMS imprinted with A_{pattern} = 120 nm fully suppressed dewetting. We anticipate a threshold crossover between these two pattern amplitudes such that 1 nm < A_{pattern} < 120 nm. PDMS patterned masks with variable amplitudes and constant pitch were fabricated by precuring the PDMS mixture for variable times (2, 4, 6, 8, 10, 12, 15, 20, and 30 min) and further curing the precured PDMS sheets on patterned templates, yielding variable amplitudes of 10, 15, 30, 45, 60, 80, 100, and 120 nm.[23] Figure 3 shows a plot of number density of dewetting holes as a function of the ratio of the initial film thickness (h) to the confining pattern amplitude (A_{pattern}). The effect of the confining pattern amplitude exhibits three regimes of film stability. In Regime 1 where the confining pattern amplitudes are greater than or equal to film thicknesses, $h/A_{\text{pattern}} \leq 1$, the density of dewetting holes is very low and the films are completely stable. This is attributed to the fact that at high pattern amplitude, the potentially growing height perturbations of even the most dominant instability mode are fully pinched-off locally, thus completely arresting the full wavelength instability and yielding stable films. In regimes 2 and 3, the pattern amplitudes (A_{pattern}) are less than film

dx.doi.org/10.1021/am4002502 | ACS Appl. Mater. Interfaces 2013, 5, 4006−4010

thickness (h), $h/A_{pattern} \geq 1$. Regime 2 transition zone occurs for $1 \leq h/A_{pattern} \leq 3$, and exhibits early stage dewetting holes whose number density (logarithmic scale, N_H) scales as $N_H \approx (h/A_{pattern})^{2.5\pm0.2}$, which is reduced from $N_H \approx h^{4.0 \pm 0.1}$ observed in unconfined films.[3] The reduced exponent reflects the partial suppression of capillary waves. In Regime 3, we have $3 \leq h/A_{pattern,}$ and we observe late stage growth and coalescence of holes as the amplitude of the capillary wave locally is not sufficiently cutoff at subcapillary wavelength scales. A phase map of the various regimes of PS film stability (Figure 4) under nanopatterned soft confinement indicates a tunable window possessing an upper limit in $\lambda_{pattern}$ and a lower limit in $A_{pattern}$ relative to λ_{cap} and h, respectively.

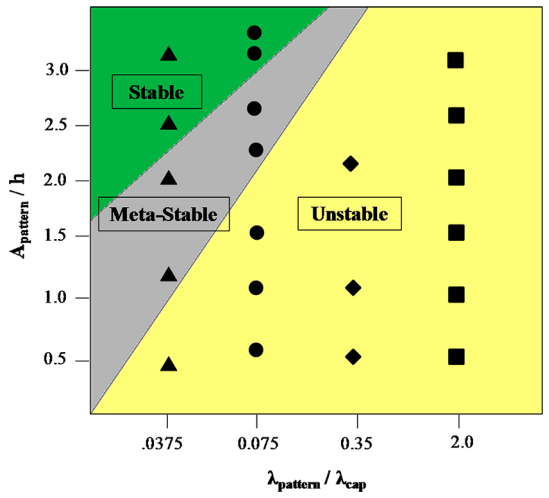

Figure 4. Stability regime phase map showing the coupled effects of confining pattern amplitude (normalized by film thickness) and wavelength on PS thin film stability.

■ ASSOCIATED CONTENT

Ⓢ Supporting Information

Large area optical micrographs of PS films of different thicknesses confined by unpatterned PDMS during thermal annealing, atomic force microscope images of patterned PS films obtained via patterned PDMS confinement. This material is available free of charge via the Internet at http://pubs.acs.org/.

■ AUTHOR INFORMATION

Corresponding Author

*Phone: (330) 972-8324. E-mail: alamgir@uakron.edu.

Notes

The authors declare no competing financial interest.

■ ACKNOWLEDGMENTS

D.B. and A.K. thank Arvind Modi, Dr. Manish M. Kulkarni, and Prof. Ashutosh Sharma for helpful discussions, and Jack F. Douglas and Sanat Kumar for a critical reading of this paper, and Rabibrata Mukherjee for sharing with us the controlled amplitude PDMS patterning technique of ref 23. This work was supported by the U.S. Department of Energy DOE-BES (Grant No. DE-FG02-10ER4779), and the Akron Functional Materials Center (AFMC).

■ REFERENCES

(1) Xia, Y.; Kim, E.; Zhao, X.-M.; Rogers, J. A.; Prentis, M.; Whitesides, G. M. *Science* **1996**, *273*, 347−349.
(2) Mukherjee, R.; Sharma, A.; Gonuguntla, M.; Patil, G. K. *J. Nanosci. Nanotechnol.* **2008**, *8*, 3406−3415.
(3) Reiter, G. *Phys. Rev. Lett.* **1992**, *68*, 75−78.
(4) Muller-Buschbaum, P. *Eur. Phys. J. E* **2003**, *12*, 443−448.
(5) Scheludko, A. *Proc. K. Akad. Wetensch. B* **1962**, *65*, 87−90.
(6) Sferrazza, M.; Carelli, C. *J. Phys. Condens. Matter* **2007**, *19*, 073102−1−073102−34.
(7) Sharma, A.; Reiter, G. *J. Colloid Interface Sci.* **1996**, *178*, 383−399.
(8) Sferrazza, M.; Xiao, C.; Jones, R. A. L.; Bucknall, D. G.; Webster, J.; Penfold, J. *Phys. Rev. Lett.* **1997**, *78*, 3693.
(9) Shull, K. R.; Mayes, A. M.; Russell, T. P. *Macromolecules* **1993**, *26*, 3929−3936.
(10) Kargupta, K.; Sharma, A. *Phys. Rev. Lett.* **2001**, *86*, 4536−4539.
(11) Suh, K. Y.; Park, J.; Lee, H. H. *J. Chem. Phys.* **2002**, *116*, 7714−7718.
(12) Barnes, K. A.; Karim, A.; Douglas, J. F.; Nakatani, A. I.; Gruell, H.; Amis, E. J. *Macromolecules* **2000**, *33*, 4177−4185.
(13) Yerulshalmirozen, R.; Klein, J.; Fetters, L. J. *Science* **1994**, *263*, 793−795.
(14) Kropka, J. M.; Green, P. F. *Macromolecules* **2006**, *39*, 8758−8762.
(15) Carroll, G. T.; Sojka, M. E.; Lei, X.; Turro, N. J.; Koberstein, J. T. *Langmuir* **2006**, *22*, 7748−7754.
(16) Seemann, R.; Herminghaus, S.; Jacobs, K. *Phys. Rev. Lett.* **2001**, *86*, 5534−5537.
(17) Suh, K. Y.; Lee, H. H. *Adv. Funct. Mater.* **2002**, *12*, 405−413.
(18) Brochard-Wyart, F.; Daillant, J. *Can. J. Phys.* **1990**, *68*, 1084−1088.
(19) Martin, P.; Brochard-Wyart, F. *Phys. Rev. Lett.* **1998**, *80*, 3296−3299.
(20) Chen, X.-C.; Li, H.-M.; Fang, F.; Wu, Y.-W.; Wang, M.; Ma, G.-B.; Ma, Y.-Q.; Shu, D.-J.; Peng, R.-W. *Adv. Mater.* **2012**, *24*, 2637−2641.
(21) Ding, Y.; Ro, H. W.; Germer, T. A.; Douglas, J. F.; Ockerberg, B. C.; Karim, A.; Soles, C. *ACS Nano* **2007**, *1*, 84−92.
(22) Julthongpiput, D.; Zhang, W.; Douglas, J. F.; Karim, A.; Fasolka, M. J. *Soft Matter* **2007**, *3*, 613−618.
(23) Bhandaru, N.; Roy, S.; Suruchi; Harikrishnan, G.; Mukherjee, R. *ACS Macro Lett.* **2013**, *2*, 195−200.